PCCP

COMMUNICATION

View Article Online
View Journal | View Issue

Cite this: *Phys. Chem. Chem. Phys.*, 2025, **27**, 18116

Received 11th June 2025,
Accepted 12th August 2025

DOI: 10.1039/d5cp02229k

rsc.li/pccp

Homoleptic magnesium and calcium complexes supported by constrained reduced Schiff base ligand for lactide polymerisation: DFT analysis of lactide/ligand interactions

Trinity Quek,[a] Thonthun Saeteaw,[a] Tanyawan Pongpanit,[a] Supawadee Namuangruk *[b] and Khamphee Phomphrai *[a]

A homoleptic calcium complex supported by a constrained reduced Schiff base ligand was synthesised and found to be highly active for the ring-opening polymerisation (ROP) of 100 equiv. lactide within 2 min at room temperature. However, the magnesium analogue has significantly lower reactivity. Single-crystal X-ray diffraction revealed a 6-coordinate metal environment for both complexes. Density functional theory (DFT) calculations showed that the calcium complex can asccommodate up to 7-coordination, thereby facilitating polymerisation without detachment of the dimethylamino sidearm, unlike in the magnesium complex. The participation of the phenoxy group and secondary amine (N–H) were observed to facilitate polymerisation *via* hydrogen bonding.

Polylactide (PLA) is a key example of a biopolymer which is both bio-sourced and biodegradable.[1,2] It has been extensively studied for its potential to replace some petrochemical-derived plastics in packaging materials.[3] Several catalyst systems for the polymerisation of lactide have been reported such as metal complexes,[4] organocatalysts,[5] and enzymes.[6,7] For ligated metal-catalysed polymerisation of lactide, the common catalyst framework is heteroleptic, comprising a metal atom coordinating to both a ligand set and an initiating group: the ligand set attached to the metal controls the reactivity and selectivity of the catalysts while the initiating group such as alkoxides or amides initiates the polymerisation.[8] The common polymerisation mechanism for heteroleptic catalysts is the coordination-insertion mechanism – the catalysts are active by themselves without added initiators. In contrast, homoleptic metal catalysts, although synthetically simpler and not prone to ligand redistribution *via* Schlenk equilibrium, are less explored in lactide polymerisation. The polymerisation mechanism typically proceeds *via* an activated monomer pathway, requiring an external initiator such as an alcohol.[9] In this mechanism, the catalyst, monomer, and initiator cooperate in the ROP process.

Several homoleptic metal complexes supported by Schiff base ligands have been reported for ROP of lactide.[10] In 2018, a range of homoleptic ethylenediamine-based magnesium and zinc complexes were reported and found to be highly active under industrially relevant conditions (*e.g.*, 10 000 equiv. lactide at 180 °C).[11] In 2021, we reported that homoleptic zinc and magnesium complexes supported by constrained reduced Schiff base ligands for the ROP of lactide at room temperature.[12] The zinc complex with reduced imine groups in the ligand was found to be significantly more active than the Schiff base analogue (1 min *vs.* 5 days under identical conditions). Therefore, the reduced Schiff base ligand system undoubtedly enhances the catalytic activities. In this study, we expanded this ligand system to calcium metal and, through DFT calculations, demonstrated that the N–H proton in the reduced ligand has significant influence on the activities of the catalyst.

The calcium complex supported by reduced Schiff base ligand is shown in Scheme 1. Key features include: a constrained five-membered ring which increases the distance between O and N(H) atoms, a reduced Schiff base containing an NH proton which may introduce hydrogen-bonding character, and a

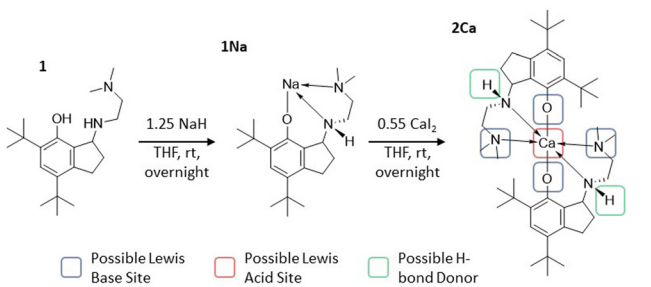

Scheme 1 Synthesis of complex **2Ca** from ligand **1**.

[a] *Department of Materials Science and Engineering, School of Molecular Science and Engineering, Vidyasirimedhi Institute of Science and Technology (VISTEC), 555 Moo 1, Payupnai, Wangchan, Rayong 21210, Thailand. E-mail: khamphee.p@vistec.ac.th*

[b] *National Nanotechnology Center (NANOTEC), National Science and Technology Development Agency (NSTDA), 111 Innovation Cluster 2 Thailand Science Park, Khlong Nueng, Khlong Luang, Pathum Thani, 12120, Thailand. E-mail: supawadee@nanotec.or.th*

dimethyl amine sidearm which may facilitate proton abstraction from the alcohol initiator. The constrained reduced Schiff base ligand **1** and the homoleptic magnesium complex **2Mg** were synthesised according to our published methods.[12] For the calcium analogue, the ligand precursor **1** was treated with NaH in THF followed by a reaction with CaI_2 resulting in a white powder of homoleptic calcium complex **2Ca** in moderate yield (Scheme 1). Complexes **2Mg** and **2Ca** were crystallised in toluene at −35 °C and characterised by single-crystal XRD as shown in Fig. 1 for **2Ca** and in Fig. S8, in the SI for **2Mg**. Both complexes were identified as bis-ligated homoleptic complexes as anticipated exhibiting a C_2 symmetry. The metal centres displayed octahedral coordination geometry, in contrast to the previously reported tetrahedral coordination observed in the zinc analogue.[12] Given the structural similarity between the calcium and magnesium complexes, they both shared the *Pbcn* space group. The crystal lattices contained co-crystalised toluene molecules for each metal complex. The phenoxy groups occupied *trans* positions, with the dimethyl amine groups in *cis*, forming N2–M–N2′ bond angles of 100.0° for **2Mg** and 106.7° for **2Ca**. Due to the larger ionic radius of calcium, the N2–N2′ distance was also greater in **2Ca** (4.094 Å) compared to **2Mg** (3.562 Å), suggesting a larger pocket around the metal centre in **2Ca**.

The polymerisation of L-lactide (L-LA) were carried out at L-LA : cat : BnOH mole ratio of 100 : 1 : 1 in dichloromethane at room temperature. Benzyl alcohol (BnOH) was added as an initiator in the reactions. Complex **2Mg** catalysed the polymerisation to 95% conversion in 30 min (Table 1, entry 1).[12] On the other hand, complex **2Ca** was significantly more active: finishing in only 2 min (entry 2). The dispersity of polylactide (PLA) resulting from **2Mg** was narrow ($Đ$ = 1.08) while that using **2Ca** was slightly broader ($Đ$ = 1.49) reflecting the faster polymerisation and transesterification rates of the calcium complex.

A polymerisation using a low [L-LA] : [**2Ca**] : [BnOH] molar ratio of 10 : 1 : 1 was carried out to identify the end group of the polymer. The result from MALDI-TOF spectrometry revealed the mass series of $BnO[LA/2]_nH + Na^+$ confirming that benzyl alcohol is the only initiator in the polymerisations (see Fig. S5 in SI). However, the mass series were spaced apart by 72 Da – half of a lactide monomer. This indicates that transesterification occurs as also indicated by the broad dispersity of the obtained polymer. Polymerisation of *rac*-lactide using **2Ca** was also carried out (entry 3) completing in only 1 min and yielding primarily atactic PLA (see Fig. S4 in SI). Complex **2Ca** is much more reactive than other related homoleptic calcium complexes supported by NNO-tridentate ketiminate ligands (without N–H moieties) containing similar NMe_2 side groups (2 min *vs.* 120 min under similar conditions).[13] Therefore, the difference in ligand backbone have significant impact on the catalytic activity.

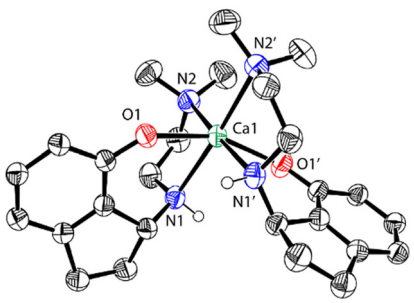

Fig. 1 Molecular structure of **2Ca** with thermal ellipsoids drawn at 50% probability level. For clarity, most hydrogen atoms and all ^{t}Bu groups are omitted. Selected bond distances (Å) and angles (deg): Ca1–O1 2.207(2), Ca1–N1 2.484(3), Ca1–N2 2.552(3), O1–N1 2.994(3); O1–Ca1–O1′ 157.8(1), O1–Ca1–N1 79.1(1), O1–Ca1–N2 96.8(1), N1–Ca1–N2′ 175.4(1).

Table 1 Polymerisation of lactide using magnesium and calcium complexes

Entry	Cat.	Lactide equiv.	Time (min)	Conv.[a] (%)	$M_{n,th.}$[b] (kDa)	$M_{n,adj.}$[cd] (kDa)	$Đ$[c]
1[e]	**2Mg**	100 L-LA	30	95	13.8	6.0	1.08
2	**2Ca**	100 L-LA	2	88	12.7	12.4	1.49
3	**2Ca**	100 *rac*-LA	1	90	13.0	6.1	1.60

Reaction conditions: $[LA]_0$ = 0.50 M, DCM, room temperature. Benzyl alcohol was added equimolar to catalyst. [a] Determined from NMR analysis of crude reaction sample. [b] $M_{n,th.} = ([LA]_0/[Cat.]_0 \times \text{conversion} \times MW_{LA}) + MW_{BnOH}$. [c] Determined by GPC analysis. [d] Adjusted by correction factors of 0.53 for entries 1, 3 and 0.59 for entry 2 (see ref. 14). [e] Data taken from our previous work in ref. 12 for comparison.

Computational studies are a powerful tool to elucidate mechanistic pathways in ROP of cyclic esters.[15,16] Previous work by Ejfler on pseudo-octahedral aminophenolate Zn complexes revealed that the dioxolane sidearm is capable to open up to accommodate the active catalyst geometry.[17] In this study, to understand why the calcium complex is significantly more active than its magnesium analogue despite both adopting 6-coordinate geometries, we conducted DFT calculations using the Gaussian 16 program [see SI for computational details].

The XRD-derived models were simplified by replacing *tert*-butyl groups with hydrogen atoms, and methanol was used in place of benzyl alcohol. Optimisation was performed using the M06-2X functional with the 6-31G(d,p) basis set while frequency was calculated at the 6-311+G(d,p) level of theory – these are suitable for studying both group(II) complexes[18] and organocatalysts.[19,20] In the absence of an initiating group such as an alkoxide or amide, the polymerisation likely proceeds *via* the activated monomer mechanism.[21,22] This involves coordination of the lactide monomer to the Lewis acid metal site followed by nucleophilic attack from benzyl alcohol.

Therefore, two distinct reaction pathways, pathways ***I*** and ***II***, outlined in Scheme 2, were proposed depending on whether the NMe_2 sidearm (pathway ***I***) or the phenolate oxygen (pathway ***II***) acts as the Lewis base. In both cases, the transition states involve proton transfer from the benzyl alcohol initiator to the lactide monomer.

The optimised geometries for the complexes in Scheme 3 are provided in the SI. The corresponding free energy profiles are shown in Fig. 2. In pathway ***I***, we found that the complex first opens one labile NMe_2 arm to form a 5-coordinate complex, **Op-Ca*I***. In the meta-stable open-arm state **Op-Ca*I***, one NMe_2 group forms a hydrogen bond with the NH proton of the ligand. In the reactant complex **Rt-Ca*I***, this NMe_2 group

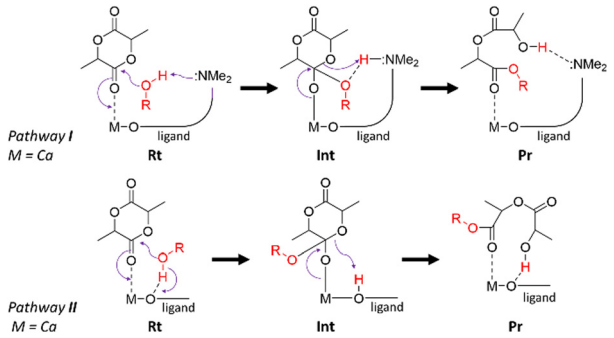

Scheme 2 Generalised reaction pathways for the ring-opening of the lactide monomer focusing on the catalyst active site.

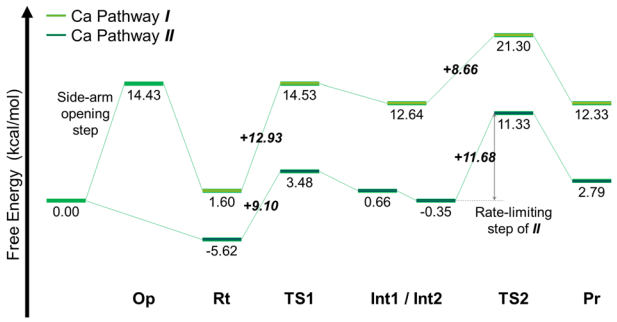

Fig. 2 Free energy profiles for calcium complex-catalysed lactide ring opening, calculated at M062X/6-311+G(d,p)//M062X/6-31G(d,p). Pathways *I* and *II* involve side-arm opening and non-opening to form 6- and 7-coordination complexes (Rt), respectively. Labels include Op (open-arm), Rt (reactant), TS (transition state), Int (intermediate), and Pr (product).

subsequently forms a hydrogen bond with methanol, while the lactide coordinates to the Ca centre. The transition state **TS1-Ca*I*** features methanol attacking the carbonyl carbon of lactide while transferring its proton to NMe_2. The resulting intermediate **Int1-Ca*I*** leads to a second transition state, **TS2-Ca*I***, where the proton rearranges to the lactide ring oxygen, facilitating ester bond cleavage and yielding the ring-opened product **Pr-Ca*I***.

In contrast, pathway ***II*** proceeds without the need to open a NMe_2 sidearm, owing to calcium's large ionic radius. This enables a stable 7-coordinate complex, **Rt-Ca*II***, where both NMe_2 groups remain attached. The initiator forms a hydrogen bond with a ligand oxygen, while the lactide monomer simultaneously coordinates to the calcium centre and the ligand's NH proton. These interactions persist through **TS1-Ca*II*** and **Int1-Ca*II***. The intermediate **Int2-Ca*II*** involves a rotation of lactide monomer to align the abstracted proton near the oxygen of ester bond (-1.01 kcal mol^{-1}). **TS2-Ca*II*** then facilitates bond cleavage, forming the final product **Pr-Ca*II*** in which the ring-opened molecule coordinates to the ligands instead of the metal. The hydrogen bond between the NH and lactide's carbonyl oxygen is unique to pathway ***II***.

The free energy profiles in Fig. 2 show that pathway ***I*** begins with a high-energy arm-opening step to form the destabilised **Op-Ca*I*** before forming **Rt-Ca*I***. Conversely, in pathway ***II***, lactide directly binds to Ca in **Rt-Ca*II*** without prior arm opening. In addition, an interaction between NH group with oxygen atom of the monomer could stabilise the coordinated species. This step has a favourable binding energy of -5.62 kcal mol^{-1}. The rate-determining transition state **TS2-Ca*II*** requires only 11.68 kcal mol^{-1}, indicating that pathway ***II*** is the more favourable route for calcium-catalysed ROP.

Similar mechanisms were evaluated for the magnesium complex **2Mg** (see SI, Fig. S11–S13). The smaller ionic radius

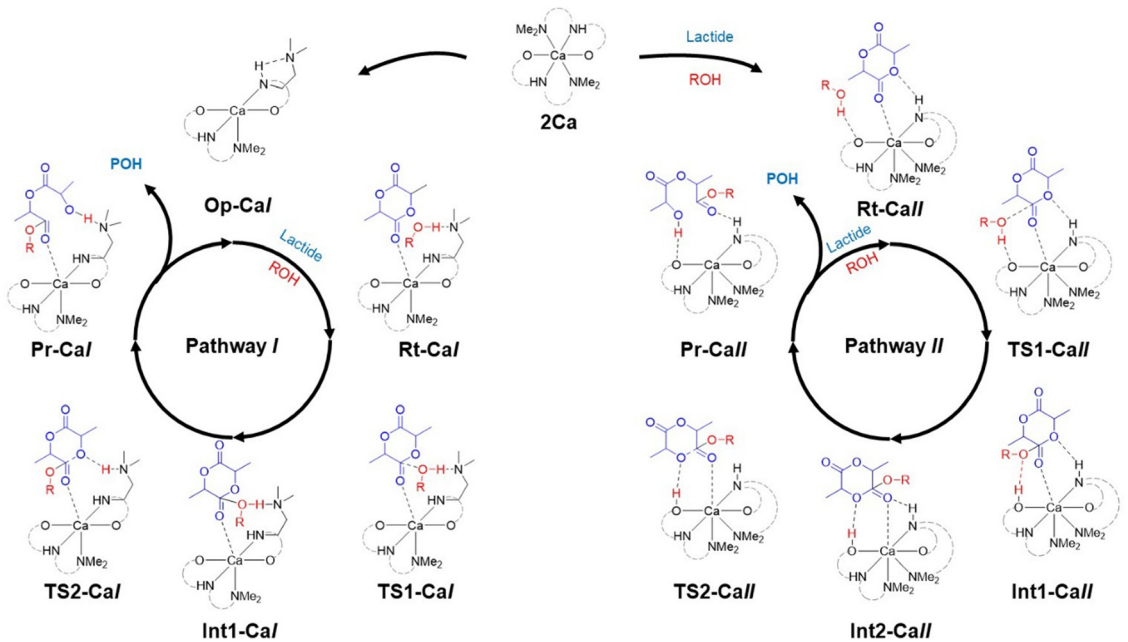

Scheme 3 Reaction pathways ***I*** and ***II*** for the calcium complex based on the optimised models obtained. R = Me in all computational experiments and POH = ring-opened product. For optimised models of all states, refer to the SI.

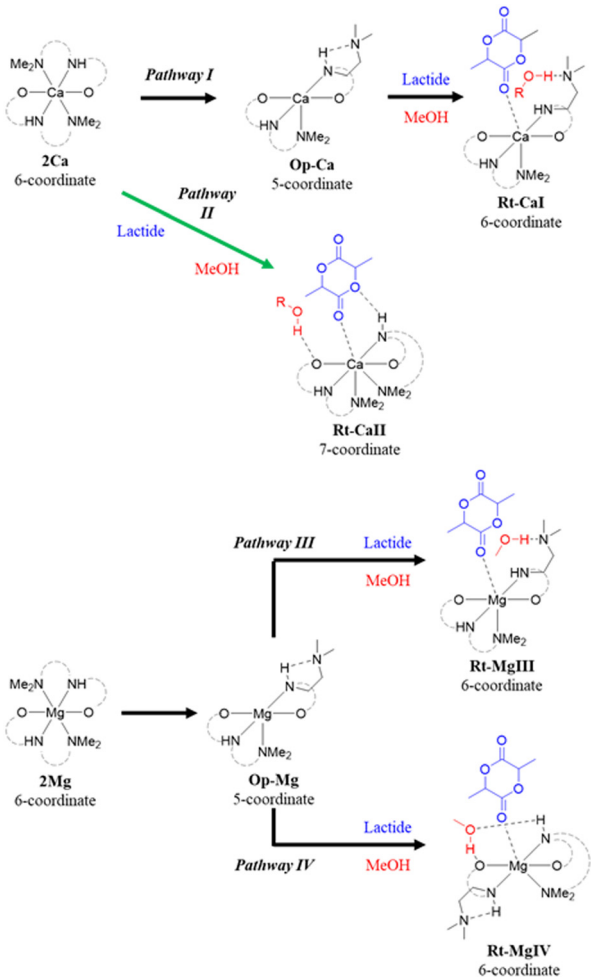

Scheme 4 Depiction of all four reactant complex formation pathways.

of Mg restricts coordination to six, necessitating NMe_2 dissociation to form a five-coordinate structure for monomer binding. Two further pathways are proposed: pathway ***III***, where NMe_2 abstracts the methanol proton, and pathway ***IV***, where the phenoxy oxygen acts as the base. Pathways ***III*** and ***IV*** for magnesium have significantly higher energy barriers. The dissociation of the NMe_2 sidearm in **Op-Mg** is required in both pathways for +15.25 kcal mol^{-1}. Therefore, the enhanced catalytic activity of the calcium complex can be attributed to its ability to accommodate lactide without sidearm dissociation, leading to the most favourable thermodynamic and kinetic reactions along with the participation of the NH group *via* hydrogen bonding (Scheme 4).

In conclusion, a homoleptic calcium complex supported by a constrained reduced Schiff base ligand derived from an indanone backbone was synthesised and structurally characterised. It exhibited significantly higher activity in lactide polymerisation compared to its magnesium analogue. DFT computational studies support this observation, revealing that the larger atomic size of calcium enables thermodynamically favourable 7-coordinate complexes without arm opening, thereby reducing the activation barrier. Additionally, phenoxy and NH interactions assist in ring-opening through hydrogen bonding, reminiscent of ligand-assisted Lewis acid organocatalysis.

Conflicts of interest

There are no conflicts of interest to declare.

Data availability

The data supporting this article have been included as part of the SI. Supplementary information available: Methods, NMR spectra, DFT models, elemental analysis, crystal data. See DOI: https://doi.org/10.1039/d5cp02229k

CCDC 2393070 and 2393071 contain the supplementary crystallographic data for this paper.[23,24]

Acknowledgements

Financial supports from VISTEC (M22KHP-VIS010), National Research Council of Thailand (no. N42 A650196), Thailand Science Research and Innovation (TSRI) (no. FRB680014/0457), and Program Management Unit for Human Resources & Institutional Development, Research and Innovation (B41G680026, Global League) are gratefully acknowledged.

Notes and references

1 M. S. Kim, H. Chang, L. Zheng, Q. Yan, B. F. Pfleger, J. Klier, K. Nelson, E. L. W. Majumder and G. W. Huber, *Chem. Rev.*, 2023, **123**, 9915–9939.
2 Y. Zhu, C. Romain and C. K. Williams, *Nature*, 2016, **540**, 354–362.
3 R. Auras, B. Harte and S. Selke, *Macromol. Biosci.*, 2004, **4**, 835–864.
4 A. B. Kremer and P. Mehrkhodavandi, *Coord. Chem. Rev.*, 2019, **380**, 35–57.
5 N. E. Kamber, W. Jeong, R. M. Waymouth, R. C. Pratt, B. G. G. Lohmeijer and J. L. Hedrick, *Chem. Rev.*, 2007, **107**, 5813–5840.
6 H. Zhao, G. A. Nathaniel and P. C. Merenini, *RSC Adv.*, 2017, **7**, 48639–48648.
7 H. Zhao, *J. Chem. Technol. Biotechnol.*, 2018, **93**, 9–19.
8 C. A. Wheaton, P. G. Hayes and B. J. Ireland, *Dalton Trans.*, 2009, 4832–4846.
9 S. Penczek and J. Pretula, *ACS Macro Lett.*, 2021, **10**, 1377–1397.
10 M. Fuchs, S. Schmitz, P. M. Schäfer, T. Secker, A. Metz, A. N. Ksiazkiewicz, A. Pich, P. Kögerler, K. Y. Monakhov and S. Herres-Pawlis, *Eur. Polym. J.*, 2020, **122**, 109302.
11 P. McKeown, S. N. McCormick, M. F. Mahon and M. D. Jones, *Polym. Chem.*, 2018, **9**, 5339–5347.
12 T. Pongpanit, T. Saeteaw, P. Chumsaeng, P. Chasing and K. Phomphrai, *Inorg. Chem.*, 2021, **60**, 17114–17122.
13 M.-W. Hsiao and C.-C. Lin, *Dalton Trans.*, 2013, **42**, 2041–2051.

14 B. Kost, M. Socka, K. Cichoń, M. Brzeziński, M. Basko and T. Biela, *Polym. Adv. Technol.*, 2024, **35**, e6296.
15 D. Jędrzkiewicz, D. Kantorska, J. Wojtaszak, J. Ejfler and S. Szafert, *Dalton Trans.*, 2017, **46**, 4929–4942.
16 I. Nifant'ev and P. Ivchenko, *Molecules*, 2019 **24**, 4117.
17 J. Wojtaszak, K. Mierzwicki, S. Szafert, N. Gulia and J. Ejfler, *Dalton Trans.*, 2014, **43**, 2424–2436.
18 C. Qi, F. Hasenmaile, V. Gandon and D. Lebœuf, *ACS Catal.*, 2018, **8**, 1734–1739.
19 M. Lalanne-Tisné, A. Favrelle-Huret, W. Thielemans, J. P. Prates Ramalho and P. Zinck, *Catalysts*, 2022 **12**, 1280.
20 G. Nogueira, A. Favrelle, M. Bria, J. P. Prates Ramalho, P. J. Mendes, A. Valente and P. Zinck, *React. Chem. Eng.*, 2016, **1**, 508–520.
21 F.-J. Lai, L.-L. Chiu, C.-L. Lee, W.-Y. Lu, Y.-C. Lai, S. Ding, H.-Y. Chen and K.-H. Wu, *Polymer*, 2019, **182**, 121812.
22 X. Li, M. Zang, L. Zhang, W. Jiang, X. Zhao, X. Jiang and W. Yao, *Organometallics*, 2024, **43**, 2862–2871.
23 T. Quek, T. Saeteaw, T. Pongpanit, S. Namuangruk, K. Phomphrai, CCDC 2393070: Experimental Crystal Structure Determination, 2025, DOI: **10.5517/ccdc.csd.cc2lb5ty**.
24 T. Quek, T. Saeteaw, T. Pongpanit, S. Namuangruk, K. Phomphrai, CCDC 2393071: Experimental Crystal Structure Determination, 2025, DOI: **10.5517/ccdc.csd.cc2lb5vz**.

